Energy & Environmental Science

ROYAL SOCIETY OF CHEMISTRY

PAPER

View Article Online
View Journal | View Issue

Cite this: *Energy Environ. Sci.*, 2024, **17**, 4248

Closing the loop: recycling of $MAPbI_3$ perovskite solar cells†

Zhenni Wu, *[ab] Mykhailo Sytnyk,[b] Jiyun Zhang,[ab] Gülüsüm Babayeva,[b] Christian Kupfer,[ab] Jin Hu,[a] Simon Arnold,[a] Jens Hauch,[ab] Christoph Brabec[ab] and Ian Marius Peters*[ab]

Closed-loop recycling is crucial in the rapidly expanding era of photovoltaic deployment. Yet, the recycling of commercial silicon photovoltaic modules presents challenges due to laborious component separation. In contrast, layers in solution-processed solar cells can be separated with relative ease through selective dissolution. In this study, we report on the recovery of every layer in a planar $MAPbI_3$ perovskite solar cell using a layer-by-layer solvent extraction approach, followed by purification or modification to restore quality. This method potentially allows for up to 99.97% recycled mass, thereby conserving resources and reducing waste. We assessed material quality by substituting each fresh material with its recycled equivalent during solar cell production. Subsequently, solar cells were fabricated with either several or all layers comprising recycled materials. Every combination yielded efficiency comparable to cells constructed exclusively with fresh materials, demonstrating the efficacy of the developed recycling process. Our mass and value analysis highlights ITO glass has the highest recycling priority and the need for circular utilization for by-product chemicals, especially cleaning agents. Techno-economic projections suggest that the proposed recycling procedure has the potential to afford substantial cost savings. In the lab, recycling could reduce material costs by up to 63.7%, in industrial manufacturing by up to 61.4%. A life cycle assessment reveals this recycling method can reduce environmental impacts.

Received 7th March 2024,
Accepted 7th May 2024

DOI: 10.1039/d4ee01071j

rsc.li/ees

Broader context

In light of the rapid growth in photovoltaic (PV) deployment, developing sustainable recycling processes for photovoltaic applications is becoming increasingly relevant to avert the potential accumulation of millions of tons of discarded solar panels. However, the recycling of current commercial PV modules is laborious and often amounts to downcycling due to the insufficient separation and treatment of mixed materials. Seen as a promising material for next-generation solar panels, perovskite solar cells can be solution processed, enabling relatively straightforward recycling through selective dissolution and separation techniques. In this context, we demonstrate the recycling of a $MAPbI_3$ perovskite solar cell by systematically substituting fresh components with recycled counterparts, leading to the assembly of cells featuring varying degrees of reused materials. Importantly, the efficiency levels of cells constructed using recycled components remained on par with those crafted from virgin materials entirely. Furthermore, an extended techno-economic analysis reveals the economic merits of the developed recycling procedures, both at laboratory and industrially relevant scales. A life cycle assessment further demonstrates that this approach can reduce environmental impacts.

1 Introduction

CO_2 emission reached a record high of over 36.8 Gt in 2022.[1] Among many energy generation methods, solar power has become increasingly relevant in the battle against climate change.[2] The solar photovoltaic (PV) industry reached a milestone of installing 1 TW cumulative capacity in 2022,[3] and the deployment of PV technologies will continue to thrive.[4] According to various projections, solar PV is anticipated to achieve a capacity of tens of terawatts by 2050.[5–7] Realizing terawatt-scale PV deployment will pose new challenges, such as the management of substantial resources. One aspect of this resource challenge is the handling of the projected tens of millions of tons of solar panels that reach their end of life.[8] End-of-life panels can be converted back to resources *via* recycling. Recognizing its environmental significance, the European Union[9,10]

[a] *Friedrich-Alexander-University Erlangen-Nuremberg (FAU), Faculty of Engineering, Department of Material Science, Materials for Electronics and Energy Technology (i-MEET), Erlangen 91058, Germany. E-mail: z.wu@fz-juelich.de, i.peters@fz-juelich.de*

[b] *Forschungszentrum Jülich, Helmholtz Institute Erlangen-Nürnberg for Renewable Energies (HI ERN), Erlangen 91058, Germany*

† Electronic supplementary information (ESI) available: Experimental methods; additional figures and tables. See DOI: https://doi.org/10.1039/d4ee01071j

as well as several countries[11–13] have implemented recycling measures. However, while recycling rates of more than 90% for current commercial PV modules have been published,[14] most of that recycling fails to conserve the quality of the recycled material and is factually down-cycling.[15] This challenge in achieving genuine closed-loop recycling stems from inadequate separation and treatment of mixed materials.[16–18] The root of this difficulty lies in the inherent 'linear lock-in' characteristic of silicon PV, which prioritizes durability over a single lifespan rather than material retention across multiple product generations.[19] However, resource extraction accounts for about 60% of global greenhouse emissions and contributes to over 90% of biodiversity loss and water stress.[19]

Halide perovskite solar cells (PSCs) are unique by featuring the fastest efficiency improvement realized for any solar cell technology.[20] In addition to being a serious contestant for the future material for high-efficiency solar panels,[21] the production method of perovskite solar cells may hold the key to solving existing recycling challenges. In contrast to silicon solar cells, perovskite solar cells can be fabricated using solution processing. By using a deposition sequence with complementary solvents, the deposition sequence can be designed to be reversible, allowing for 'subtractive manufacturing'. Furthermore, a life cycle assessment from Tian *et al.* has revealed that recycling perovskite solar modules can reduce energy payback time by 72.6% and greenhouse gas emission factor by 71.2%.[22] Notably, the best recycled module design can achieve a shorter energy payback time and a lower greenhouse emission factor than silicon PV.

Several studies have already demonstrated that materials in PSCs can be selectively dissolved and separated with relative ease. Transparent conductive oxide glass substrates (TCO, in some cases, together with the neighboring layer, electron transport layer or hole transport layer) were recovered and then reused to construct new cells by washing off other layers with organic solvents.[23–26] The efficiencies of the cells with recycled (electron transport layer coated) TCO are comparable to those with virgin materials.[23–26]

Going one step further, some studies also put a focus on the recovery and recycling of lead. Zhang *et al.* comprehensively categorized the developed lead recycling methods into four types: *in situ* regeneration, electrochemical deposition, adsorption–desorption and solvent extraction.[27] Noteworthy contributions in the *in situ* regeneration category includes the work of Xu *et al.*, who accomplished *in situ* recycling of PbI_2 and TiO_2 coated FTO by spin coating methylammonium iodide (MAI) solution on the surface of degraded $MAPbI_3$, which had been converted to PbI_2 fully.[28] Their recycled device presented a marginally superior efficiency than the pristine device. Poll *et al.* demonstrated electrochemical deposition for recycling lead from perovskites using deep eutectic solvents, which is yet to be studied in full devices.[29] Relevant adsorption–desorption research includes the studies conducted by Chen *et al.*[30] and Zhang *et al.*[31] Chen *et al.* successfully separated Pb from decommissioned perovskite solar modules using renewable ion exchange resins, followed by Pb precipitation to PbI_2 for the reconstruction of perovskite solar devices, which delivered similar efficiencies to their fresh counterparts.[30] Zhang *et al.* extracted lead ions from carbon-based perovskite solar cells with *N*,*N*-dimethylformamide (DMF).[31] Subsequently, the obtained lead lixivium formed $Pb(OH)_2$ precipitates with $NH_3 \cdot H_2O$, followed by conversion to PbI_2 with HI. The cell efficiency using recycled PbI_2 was modestly lower than that with virgin materials. Solvent extraction was exemplified by several works. Binek *et al.* collected PbI_2 with DMF from perovskite solar cells and carried out cooling crystallization with water, enabling the regeneration of solar cells with recycled PbI_2 and with recycled FTO substrates, both exhibiting similar efficiencies to the devices with fresh materials.[32] Feng *et al.* employed butylamine to liquefy the perovskite layer, separating it from the rest, and built solar cells with the extracted PbI_2 even with a small performance improvement.[33] Notably, Wang *et al.* recovered all the layers with a 'one solution for all' approach using a methylamine in THF solution: methylamine liquefied $MAPbI_{3-x}Br_x$ whereas THF dissolved hole transport layer (HTL) spiro-OMeTAD.[34] The two mixed liquids required overnight settling for separation. By utilizing recycled materials, supplemented with additional virgin gold, the solar cell yielded an efficiency that was 99% as high as that of a cell made entirely from virgin materials. The recycling approach developed there is effective, but comparably time consuming, suggesting the need for further refinement to speed up the process.

Overall, the aforementioned reports have rightly focused on retaining efficiencies comparable to fresh material devices (as summarized in Table S1, ESI†), as maintaining performance is one crucial aspect for assessing recycling methods. However, examining the device fabrication costs associated with using recycled components would provide additional valuable insight. This economic perspective will be important for fully determining the viability of these recycling processes moving forward. In addition to examining the efficiencies of cells utilizing recycled materials, Chen *et al.* presented the cost of recycling a 1 m^2 module in comparison to the material cost of the virgin module.[30] However, the costs of solvents required for device fabrication were omitted, leaving potential to an enhanced capturing of the total cost of a virgin module. Additionally, examination of manufacturing costs for a module incorporated with recycled materials would shed more light on the overall cost reduction achieved through recycling.

In this work, we present the recovery of every layer in a planar $MAPbI_3$ perovskite solar cell with a layer-by-layer solvent extraction approach. This approach offers an advantage over the 'one solution for all' method by eliminating the need for additional component isolation. Subsequent to component extraction/separation, we carried out purification or modification on the collected materials, leading to the recycled products. The qualities of the recycled products were then assessed by the performance comparisons between solar cells constructed with virgin materials exclusively and the ones with varying degrees of recycled materials. Moreover, we estimated the cost to manufacture a 1 m^2 module using recycled components based on our recycling process, at both lab and industrial

scales. The estimation accounted for recycling yields and cost modeling for a 1 m^2 module using only virgin materials, including solvents, for processing. This allowed a straightforward evaluation of the economic feasibility of the developed recycling process at the lab scale and its potential scalability to industrial levels. Additionally, a life cycle assessment evaluated the environmental impacts of the recycling approach.

2 Results

Fig. 1 outlines the sustainable lifecycles of perovskite solar cells, from production to recycling. The production involves multi-step processing: starting from raw materials, such as PbI_2, which reacts with MAI to form component $MAPbI_3$. Subsequent coating and annealing yield the active layer $MAPbI_3$. Material inputs impact the environment more than processing.[19] Also, several techno-economic analyses highlight materials as the primary capital input in PSC production.[35–37] Therefore, recycling materials at any stage is crucial for reducing environmental impacts and preserving embedded capital; the tighter the loop correlates with fewer environmental effects and greater conservation of capital. Faulty and retired solar cells should re-enter the production cycle through recycling, promoting a closed-loop system. Recycling involves two key processes: recovery of materials, *i.e.*, material retrieval, and their subsequent purification or modification to ensure quality. This work focuses on the recycling of all layers, except for gold electrodes, which was only recovered with limited amount due to the wasteful nature of thermal evaporation in laboratory settings.

The architecture of the perovskite solar devices utilized for recycling in this work is ITO/SnO_2/$MAPbI_3$/spiro-OMeTAD/Au. The selection of this specific stack can be attributed to the following reasons: (1) utilizing a single-cation $MAPbI_3$ without dopants and addition of passivation layer simplifies the composition and streamlines recycling; (2) ITO glass, SnO_2 and spiro-OMeTAD were selected due to their widespread use in the perovskite solar cell field, enhancing the broader applicability and transferability of their corresponding recycling methodologies; (3) spiro-OMeTAD is a prevalent HTL in record efficiency cells; (4) this stack allows selective removal and harvesting of all materials.

The recycling process sequence is outlined in Fig. 2. Fig. S1 (ESI†) presents the appearance of a cell subsequent to consecutive recycling steps. Two types of devices were assembled: one is a common small area functional cell fabricated with spin coating; another is the bigger pseudo-module (without Au electrode) prepared with doctor blading or drop casting[38,39] (the references demonstrate the optimization of drop casting technique in our lab), since using spin coating for cell preparation would result in a significant amount of material waste. Leveraging materials from larger devices enables ample recycled resources for a single device. In addition, they better mimic the modular design that industry will be moving towards, essential for translating lab demonstrations to industrial scalability. Hence, it is sensible to develop recycling procedures with modules in mind. The pseudo modules were used to harvest the HTL spiro-OMeTAD and the active layer $MAPbI_3$. On the other hand, ITO/SnO_2 and Au were collected from functional cells. The cells and the modules underwent the same procedures: they were first immersed in chlorobenzene to remove or collect spiro-OMeTAD (step I)—an indicator for

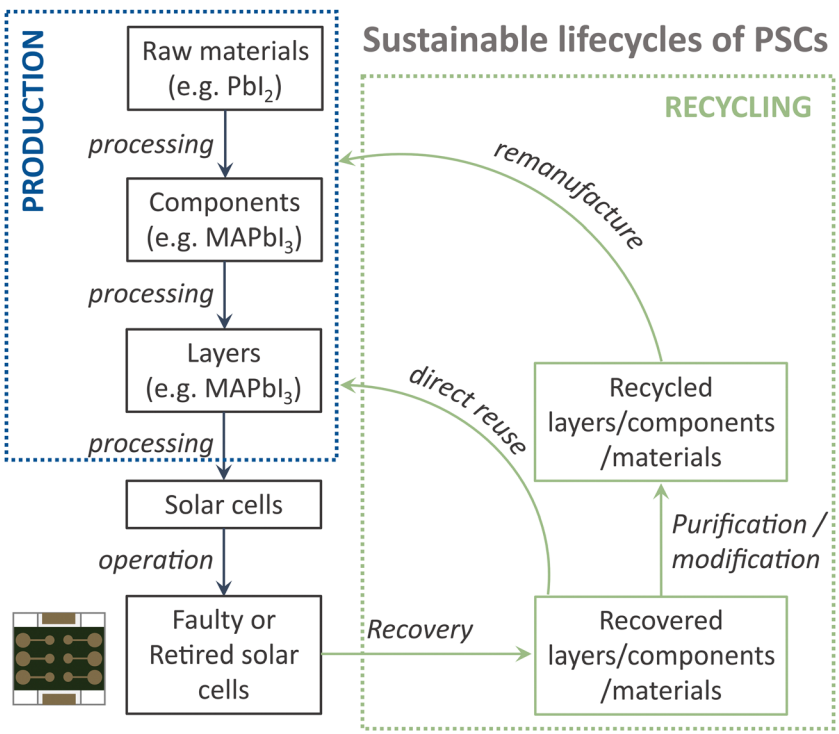

Fig. 1 Sustainable lifecycles of perovskite solar cells.

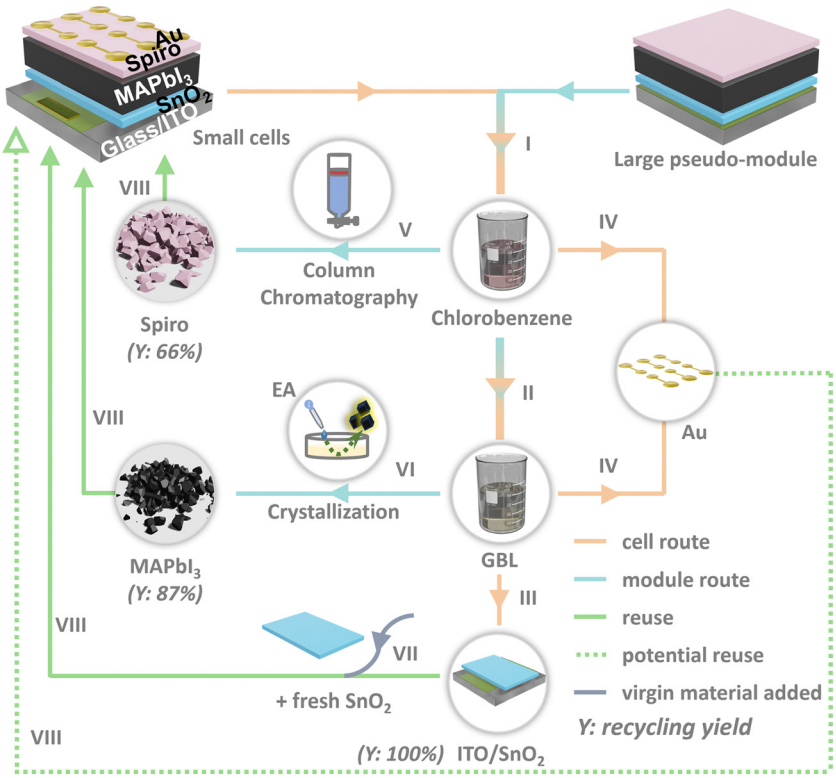

Fig. 2 Schematic diagram of closed-loop recycling of perovskite solar devices. (I) Immersion of small cells or a large pseudo-module in chlorobenzene. (II) Immersion of cell/module without spiro-OMeTAD in γ-butyrolactone (GBL). (III) Extraction of ITO/SnO_2. (IV) Filtration of Au. (V) Purification of collected spiro-OMeTAD *via* column chromatography. (VI) Purification of collected $MAPbI_3$ *via* anti-solvent crystallization, with ethyl acetate (EA) as the anti-solvent. (VII) Deposition of fresh SnO_2 on recovered ITO/SnO_2. (VIII) Cell fabrication using recycled materials. The cell route signals materials derived from cells, while the module route indicates materials derived from modules.

complete removal is the gradual fading of the greenish color on the surface (Fig. S1, ESI†), then treated with γ-butyrolactone (GBL) to salvage $MAPbI_3$ (step II)—this step should be done in a glovebox to minimize exposure to air and thus iodine loss. Simultaneously, Au was detached from SnO_2-coated ITO glass due to the dissolution of layers in between (step III and IV). In this way, we were able to obtain every individual component from a whole device.

2.1 Recycling of spiro-OMeTAD

The spiro-OMeTAD HTL in the devices (functional cells and pseudo-modules) was deposited using spiro-OMeTAD solutions doped with *t*BP, Li-TFSI, and FK209 Co(III) TFSI, as detailed in Section S1.2 (Solution preparation) of ESI.† After disassembly, the collected hole transport material (HTM) mixture was purified by column chromatography as an attempt to remove impurities, including the dopants (step V). The eluent for column chromatography was evaporated with a rotary evaporator. The remaining product is recycled spiro-OMeTAD with a recycling yield of 66%. Drop-casting spiro-OMeTAD onto pseudo-modules eliminates material waste during deposition, *i.e.* the mass on the stack equals the input mass. Thus, the recycling yield was determined by comparing the mass of obtained recycled spiro-OMeTAD to the initial input mass of fresh spiro-OMeTAD.

To obtain a preliminary assessment of the product's purity, we conducted thin-layer chromatography. The results (shown in Fig. S2a–c, ESI†) indicated the presence of only spiro-OMeTAD in the column-purified solution. However, the post-rotary evaporation product exhibited a deep reddish-brown color, as illustrated in Fig. S2d (ESI†). This color closely resembled that of doped spiro-OMeTAD solutions (Fig. S2e, ESI†), in contrast to the light yellow hue of pure spiro-OMeTAD. The reddish brown tint emerges only upon the addition of orange FK209 Co(III) TFSI to spiro-OMeTAD solutions. This observation implies that the recycled spiro-OMeTAD retains residual additives, possibly due to the chemical bonds the additives formed with spiro-OMeTAD.[40] Nevertheless, the recycled spiro-OMeTAD was further used for solar cell fabrication the same way as for fresh spiro-OMeTAD, the same number of additives were added into the recycled spiro-OMeTAD, followed by current density–voltage measurements. We believe this is a straightforward and comprehensive way to evaluate the quality of recycled materials. Processing losses and incomplete recycling yields created a deficit between the required amounts for fabrication of a cell and recycled amounts from a cell, which was addressed by supplementing with additional recycled material. This ensures an equitable comparison between recycled and their virgin counterparts. As shown in Fig. 3a, the device made with virgin materials and the one with recycled spiro-OMeTAD

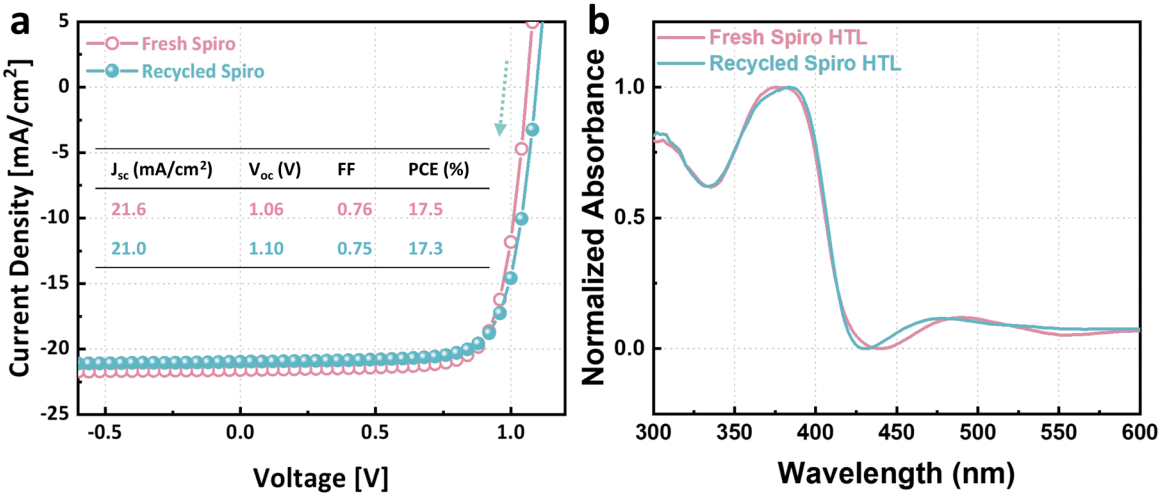

Fig. 3 Recycling of spiro-OMeTAD: (a) *JV* curves of perovskite solar cells using only fresh materials and recycled spiro-OMeTAD; (b) UV-Vis spectra of fresh and recycled spiro-OMeTAD HTL (with additives) deposited on ITO glasses. The peak around 380 nm is assigned to spiro-OMeTAD, the small peak near 480 nm stems from oxidized spiro-OMeTAD.

delivered champion power conversion efficiencies of 17.5% and 17.3%, respectively—indistinguishable within typical uncertainties. The actual PCE is estimated with an uncertainty of ±3.22% from the measured value; the derivation process is detailed in the ESI.† Their short circuit currents, open circuit voltages, and fill factors were similar as well (compare inset table in Fig. 3a), indicating that the recycled spiro-OMeTAD has satisfactory properties and did not limit device performance. Additionally, Fig. S3 (ESI†) presents the statistical distribution of photovoltaic parameters for 12 solar cells using virgin materials compared to 12 with recycled spiro-OMeTAD. While the retained excess dopants did not impact device performance significantly, this complication highlights the need to design recyclable photovoltaics carefully. Recycling doped layers might require more sophisticated processes than single-component layers.

The normalized UV-Vis spectra of a fresh spiro-OMeTAD HTM film and a recycled spiro-OMeTAD HTM film are shown in Fig. 3b. Both HTM films were prepared with their respective doped spiro-OMeTAD solutions. Two spectra exhibit resembling absorption peaks. The peak around 380 nm is attributed to spiro-OMeTAD. Another weaker peak near 480 nm is a close match to the peak of oxidized spiro-OMeTAD.[41] Oxidized spiro-OMeTAD is crucial for achieving higher efficiencies. The oxidation process is expedited by additives Li-TFSI and FK209 Co(III) TFSI (*t*BP is mainly for morphology control).[42] This oxidation induces p-doping in spiro-OMeTAD by forming spiro-OMeTAD$^+$, thereby increasing the concentration of majority charge carriers and improving the conductivity of this semiconductor. Consequently, device performances can be enhanced.[42]

2.2 Recycling of $MAPbI_3$

We subsequently investigated the recycling of $MAPbI_3$. Anti-solvent, ethyl acetate, was employed to crystallize $MAPbI_3$ from GBL collected $MAPbI_3$ solution (step VI). The yield, calculated in the same manner as for spiro-OMeTAD, was documented to be 87%. The obtained recycled $MAPbI_3$ was used to prepare functional solar cells. Current–voltage measurements show that the champion device utilizing recycled $MAPbI_3$ exhibited a comparable performance to that of the one fabricated using virgin materials (Fig. 4a). Furthermore, utilizing recycled counterparts for both active layer and hole transport layer did not lead to a significant performance loss either. We recognize a trend towards lower efficiency as more recycled materials are added to the stack. We cannot answer yet, whether this is a coincidence or points to an issue with our recycling procedure. Moreover, Fig. S4 (ESI†) displays the statistical distribution of photovoltaic parameters among three groups of 12 solar cells each: those made with virgin materials, those using recycled $MAPbI_3$, and those incorporating both recycled $MAPbI_3$ and spiro-OMeTAD.

X-Ray diffraction (XRD) patterns of fresh $MAPbI_3$ and recycled $MAPbI_3$ were also compared, shown in Fig. 4b. Both samples demonstrated identical peak positions belonging exclusively to tetragonal (β) $MAPbI_3$ phase. Fig. S5 (ESI†) displays the superimposed XRD patterns between the two samples, revealing a difference in the intensities of the preferred peaks corresponding to the (110) and (220) crystal plane orientations. The diminished intensity of these peaks in the recycled $MAPbI_3$ suggests a reduced crystallinity compared to the fresh $MAPbI_3$. Furthermore, the lower relative intensity of the (110) to (200) in the recycled sample may indicate an altered crystallographic orientation.

We further conducted time-integrated photoluminescence (TI-PL) and time-resolved photoluminescence (TR-PL) to analyze the optoelectronic properties of the recycled $MAPbI_3$ films. The TI-PL spectra reveal that the PL peaks of fresh $MAPbI_3$ and recycled $MAPbI_3$ were nearly identical, located at 775 nm and 772 nm, respectively (Fig. S6, ESI†). TR-PL results are shown in Fig. 4c. We implemented a bimolecular-trapping–detrapping model within a Bayesian optimization-based fitting algorithm to fit the TR-PL results. This model, as detailed in the work of Péan,[43] and our fitting procedure, consistent with the methodology described by Kupfer,[44] facilitate a robust analysis. The

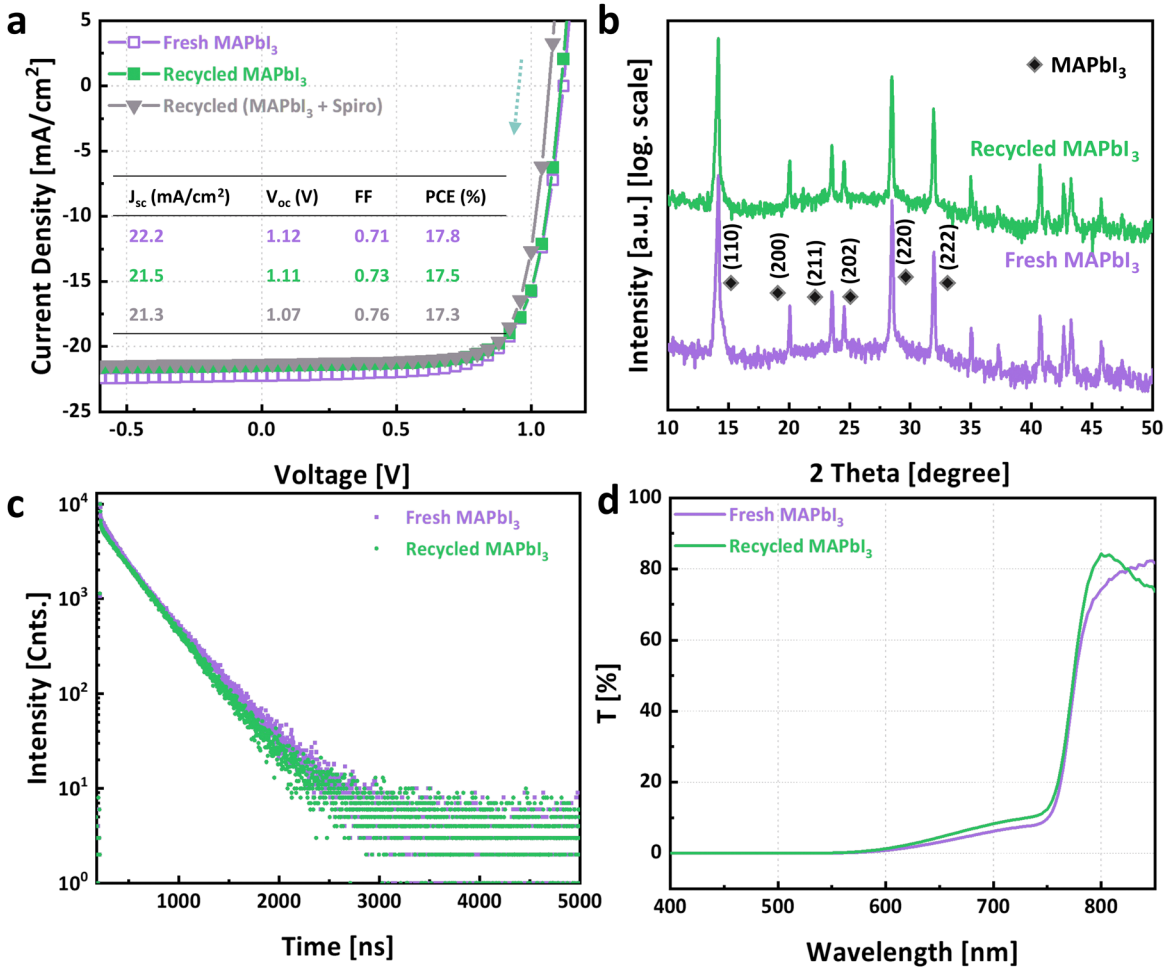

Fig. 4 Recycling of $MAPbI_3$: (a) *JV* curves of perovskite solar cells using only fresh materials, recycled $MAPbI_3$, and recycled $MAPbI_3$ and spiro-OMeTAD; (b) XRD patterns; (c) TR-PL spectra; (d) UV-Vis spectra of fresh and recycled $MAPbI_3$ films on common glasses.

fitting extracts information on the recombination of excited charge carriers. This includes band to band recombination rate constant (κ_B), trapping rate constant (κ_T), trap-assisted recombination rate constant (κ_D), and trap densities (N_T). The fitted spectra are shown in Fig. S7 in the ESI.† The corresponding fitting results are listed in Table 1. The results reveal that the band to band and trap-assisted recombination rate constant are similar for the two samples. However, both the trapping rate constant and the trap densities in the recycled $MAPbI_3$ film are marginally higher than in their fresh counterparts. Nonetheless, in terms of device performance, virgin and recycled materials do not exhibit significant differences, underscoring the defect tolerance of $MAPbI_3$, a well-established characteristic of this halide perovskite.[45,46]

UV-Visible spectroscopy sheds light on the optical characteristics of the fresh and recycled perovskite films, as shown in Fig. 4d. We observe that both samples exhibit minimal light transmission below 600 nm. Subsequently, transmittance gradually increased, although recycled $MAPbI_3$ displayed slightly higher transmission compared to the fresh counterpart. Notably, in contrast to the fresh $MAPbI_3$, the transmittance of recycled $MAPbI_3$ began to decline beyond 800 nm. However,

Table 1 TR-PL fitting results for fresh and recycled $MAPbI_3$ films. I_{PL} is a scaling factor. σ_{low} and σ_{high} are the lower and upper bounds of the standard deviation, respectively

	Fresh $MAPbI_3$			Recycled $MAPbI_3$		
	Value	σ_{low}	σ_{high}	Value	σ_{low}	σ_{high}
I_{PL} [a.u.]	1.52×10^{-25}	4.04×10^{-27}	4.15×10^{-27}	2.06×10^{-25}	6.56×10^{-27}	6.78×10^{-27}
κ_B [$m^3\ s^{-1}$]	9.19×10^{-17}	4.82×10^{-19}	4.85×10^{-19}	8.68×10^{-17}	4.23×10^{-19}	4.25×10^{-19}
κ_T [$m^3\ s^{-1}$]	3.21×10^{-14}	1.13×10^{-15}	1.17×10^{-15}	4.49×10^{-14}	1.76×10^{-15}	1.83×10^{-15}
κ_D [$m^3\ s^{-1}$]	5.25×10^{-20}	9.87×10^{-21}	1.22×10^{-20}	4.99×10^{-20}	3.82×10^{-21}	4.14×10^{-21}
N_T [m^{-3}]	$2.75 \times 10^{+22}$	$3.04 \times 10^{+20}$	$3.07 \times 10^{+20}$	$3.19 \times 10^{+22}$	$2.47 \times 10^{+20}$	$2.49 \times 10^{+20}$

since this range falls below the bandgap, the difference is expected to have a negligible impact on a solar device. Overall, recycled $MAPbI_3$ presented features with high similarity to that of fresh $MAPbI_3$, effectively empowering perovskite solar cells to rival the performance achieved using pristine $MAPbI_3$. However, it is important to recognize that the properties of recycled $MAPbI_3$ are not identical to those of virgin $MAPbI_3$. This observation suggests a tolerance in perovskite solar cells for variations in material quality.

2.3 Recycling of ITO/SnO_2 and Au harvesting

The collected ITO/SnO_2 from old cells that had been stored in a glovebox, after cleaning with ethanol, was directly reused to construct a new solar cell. As SnO_2-coated ITO glass was collected and reused as a single unit, the yield was 100%. From Fig. 5a, we observe a decrease in fill factor, leading to a reduced power conversion efficiency of 14.1%. Comparing scanning electron microscope (SEM) images, we observed distinct differences between the fresh ITO/SnO_2 substrate (Fig. 5b) and the recovered ITO/SnO_2 (Fig. 5c and d). The recovered ITO/SnO_2 exhibited evident surface damage (Fig. 5c), and a higher concentration of particles (Fig. 5d), which are highly likely to be agglomerated SnO_2. To make use of the recovered ITO/SnO_2, we added an additional layer of fresh SnO_2 on top (step VII). As shown in Fig. 5e, the surface of the sample became homogenous and did not exhibit apparent defects. Current–voltage results of a device using fresh SnO_2 coated ITO/SnO_2 that had been recovered (denoted as recycled ITO/SnO_2) show that a fresh layer of SnO_2 can restore the fill factor to the original state. The performance restoration achieved solely through the addition of SnO_2 suggests that, prior to this intervention, the ITO layer had been intact and free from damage. We conducted a two-cycle recycling process of ITO/SnO_2 to evaluate the effects of SnO_2 supplementation on series resistance. The *JV* results in Fig. S8 (ESI†) demonstrate that a second SnO_2 supplementation did not significantly alter the series resistance. Moreover, combining all the recycled materials retained the efficiency at 17%. Fig. S9 (ESI†) illustrates the statistical distribution of photovoltaic parameters for the four groups, each comprising 12 solar cells.

When dissolving the two layers between ITO/SnO_2 and Au, Au was detached from the solar cells and it remained in solution. Gold flakes could then be collected *via* filtration. Fig. 6 shows the gold filtered from the remaining chlorobenzene and GBL solutions. A small fraction of Au precipitates into the chlorobenzene solution, with the quantity varying between samples for reasons yet to be determined, as illustrated in Fig. S10 (ESI†). The majority of gold precipitated in GBL. Gold stripes at the edges of the sample did not precipitate due to their direct contact with the ITO (right subfigure in Fig. S1, ESI†). While quantifying the recovery rate of gold exactly is challenging due to the small amount needed to contact a cell, estimates based on the designed dimensions of gold contacts (Fig. S11a, ESI†) suggest that the total and edge gold areas on a sample are 173.1 mm^2 and 54 mm^2, respectively, allowing for a 68.8% recovery rate. With a coated thickness of 30 nm and a gold density of 19.32 g cm^{-3}, the recyclable gold amounts to 0.069 mg from an initial 0.1 mg per sample. The recovery rate appears to be reasonably high. However, the thermal evaporation process in our laboratory, which necessitates around 500 mg of gold to achieve a 30 nm coating, accommodates only 18 samples per batch, resulting in 99.6% of the input gold being wasted in the evaporation chamber. In Fig. S11b (ESI†), we depicted the mass flow of gold per batch from input to recycling, revealing an overall mass loss of 99.8%. Consequently, gold recovery from 417 batches is required to accumulate enough for one batch relying solely on recycled gold. In principle, the recovered gold flakes can be combined with virgin gold in the target for evaporation. However, given the extensive material losses during gold deposition, we did not proceed with this, as we could not claim that any recovered gold would end up on a recycled solar cell. Therefore, future research should prioritize

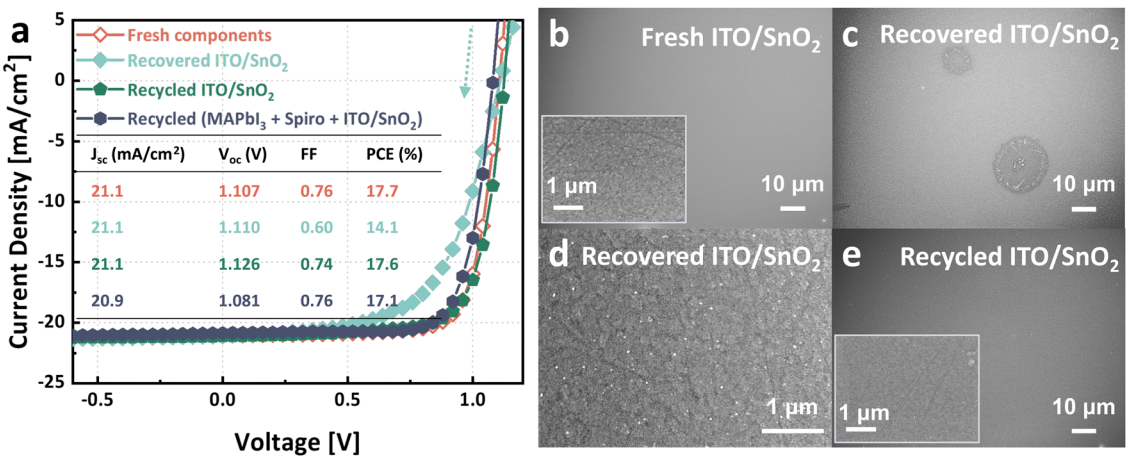

Fig. 5 Recycling of ITO/SnO_2: (a) *JV* curves of perovskite solar cells made with fresh materials, recovered ITO/SnO_2, recycled ITO/SnO_2 (recovered ITO/SnO_2 deposited with fresh SnO_2), and recycled $MAPbI_3$, spiro-OMeTAD and ITO/SnO_2; (b)–(e) SEM of (b) fresh ITO/SnO_2, (c) and (d) recovered ITO/SnO_2 and (e) recycled ITO/SnO_2. Damage and higher concentration of agglomerated SnO_2 were found on the recovered ITO/SnO_2, leading to lower efficiency, which was restored by adding a fresh layer of SnO_2.

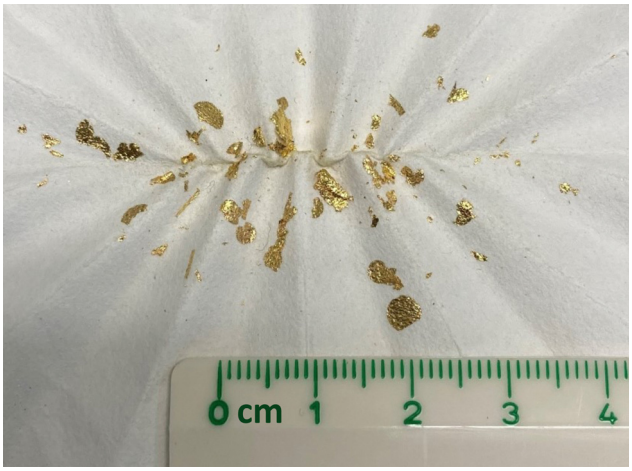

Fig. 6 Collected Au after filtration from filtrates.

the retrieval of electrode materials that accumulate in evaporator chambers, facilitating more effective recycling strategies.

3 Discussion

3.1 Recycling priorities

The goal of this study was to demonstrate a procedure that allows recovery and closed-loop recycling of all components of a perovskite solar cell. In the previous section, we have shown that it is possible to retrieve all materials and process them in a way such that they can be used to make a new solar cell without significant loss in material quality and device efficiency.

Further insight into economic and sustainability priorities in the recycling process can be gained by looking at the value and mass distribution for all components used in solar cell processing. For this purpose, we have compiled a table that documents our usage of all materials used in the fabrication process as well as the corresponding costs, and have scaled it to the fabrication of a module with 1 m^2 area. Results are shown in Table 2; numbers are a combination of our own documentation and published ones for processes that can be considered standard procedures. This table encompasses not only the primary materials of the solar panel but also ancillary materials such as solvents and cleaning agents. Note that this compilation is representative of a lab device, which is many times more expensive than an industrial process would be.

Examining the value and mass distribution (Fig. 7) provides a sense of priorities. ITO glass accounts for more than half of the value and makes up most of the mass (99.9%) of the module. Reusing the substrate, hence, has a big impact on both the economic viability as well as the sustainability balance of the cell. This aligns with the report from Tian *et al.*, which identified TCO substrates as a major contributor to both energy payback time and greenhouse gas emission factors.[22] Yet, given the reliance on indium, a critical material with limited availability, in the production of ITO glass, it is advisable to consider alternative materials such as FTO glass. FTO presents a more sustainable option, not only due to the abundance of its constituents but also because of its recyclability, which has been demonstrated in several studies.[19] Gold, being a costly and critical raw material, would be avoided in commercial PSCs. It would likely be replaced by carbon, which is more abundant in nature. Additionally, the recyclability of lead and ETL coated TCO glass in carbon-electrode PSCs has been demonstrated.[31] However, the necessity and feasibility of recycling the carbon electrode itself remains an area for further investigation. The current market price for spiro-OMeTAD is high. A more efficient and scalable preparation method, such as the one proposed by Mattiello *et al.*,[49] should be adopted to reduce costs. Nonetheless, given its complex structure, spiro-OMeTAD is likely to retain a relatively sophisticated synthesis route. Therefore, the recycling of spiro-OMeTAD is crucial. $MAPbI_3$, though contributing the third highest mass, holds limited commercial value. The feasibility of profitable recycling of $MAPbI_3$ material alone appears challenging with its overall low mass of 1.5 g m^{-2}. Lead emissions, even under severe conditions such as acid rain or catastrophic utility-scale failures, are projected to be either moderate relative to background levels or below EPA regulatory limits.[19] However, it is important to note that existing background lead levels are solely due to human activities, as there is no natural background lead.[19] Even trace levels of lead pose a risk of bioaccumulation in food chains, potentially leading to serious health hazards.[19] Consequently, the presence of lead might necessitate recovery processes as a prerequisite for the commercialization of this technology. SnO_2, finally has the smallest contribution to both mass and value. An additional thin SnO_2 layer, as required in the process we demonstrated here, may therefore be bearable and only reduces the overall recycling efficiency by a small amount.

Apart from the primary materials that have been recycled, Table 2 also draws attention to the ancillary chemicals utilized in cell processing. Based on the compiled numbers, Fig. 8 compares the mass and value of the solvents required for cell processing and the materials used in the cell itself. Cleaning agents like acetone and isopropanol but also water contribute most to mass. In terms of cost, in the process described here chlorobenzene and *t*BP are the largest contributors among solvents, though solvents only account for a fraction compared to the cell materials. However, it should be noted that most of the solvents utilized in cell processing are hazardous. DMF and NMP both have been identified as reproductive toxins,[50,51] while chlorobenzene is highly toxic to aquatic organisms with lasting repercussions and leads to serious irritation of the eyes.[52] Recycling hazardous substances can reduce their ecological impact. A more effective closed-loop system also demands the recycling of ancillary materials used in production. Therefore, developing processes that use solvents with minimal footprint and their recycling will be an important next step in the development of fully recyclable solar cells.

3.2 Techno-economic assessment of the proposed recycling method

Lab-scale recycling. A recycling process should not only be evaluated based on the quality of recycled materials, but also on

Table 2 Mass and value inventory scaled for a perovskite module with 1 m^2 area based on our fabrication sequence with an active area of 70%. Usage number was adapted from lit;[47,48] it is assumed that 3 mL 2.5% SnO_2 is required (3 mL is the overall volume for the solvent of perovskite solution in ref. 47). The pricing was derived from our laboratory's procurement data (the source of the materials can be found in the ESI), with the exchange rate of 1 euro equivalent to 1.08 dollars, with an exception of the price of H_2O[35] and the price of Au (market price on June 10, 2023). NMP: *N*-methyl-2-pyrrolidone

Layer	Material	Usage[47,48]	Price ($) [$P_V$]	Subtotal cost ($) [$C_{VC}$]	Total cost per layer ($) [$C_{VL}$]	Density (g mL^{-1})	Subtotal mass (g) [M_o]	Total mass per layer (g)
ITO glass	ITO glass	1 m^2	243.74	243.74	244.30	—	5000	5084.57
	Deionized water	33 mL	0.012/L[35]	0.0004		0.997	32.90	
	Acetone	33 mL	83.88/10 L	0.28		0.7844	25.89	
	Isopropanol	33 mL	85.17/10 L	0.28		0.7812	25.78	
SnO_2	SnO_2 (15%)	0.58 g	88.29/500 g	0.10	0.17	1.153	0.58	2.81
	Deionized water	1.25 mL	0.012/L[35]	0.00002		0.997	1.25	
	Isopropanol	1.25 mL	28.78/500 mL	0.072		0.7812	0.98	
$MAPbI_3$	MAI	0.14 g	75/10 g	1.05	7.62	—	0.14	4.56
	PbI_2	1.38 g	359/100 g	4.95		—	1.38	
	DMF	2.4 mL	126.13/250 mL	1.21		1.028	2.47	
	NMP	0.6 mL	169.25/250 mL	0.41		0.9445	0.57	
Spiro-OMeTAD	Spiro-OMeTAD	0.774 g	83/1 g	64.24	79.01	—	0.77	13.47
	LiTFSI	0.097 g	49.91/5 g	0.97		—	0.10	
	FK 209 Co(III) TFSI	0.092 g	306.15/5 g	5.63		—	0.09	
	Acetonitrile	0.495 mL	152/250 mL	0.30		0.786	0.39	
	Chlorobenzene	10.7 mL	137.98/250 mL	5.91		1.106	11.83	
	*t*BP	0.284 g	172.48/25 g	1.96		—	0.28	
Au	Au	1.65 g	63.04/g	104.02	104.02	—	1.65	1.65

economic feasibility. Thus, we also considered the chemical consumption and cost of our recycling process projected for a 1 m^2 solar module. Note that this study focuses solely on material costs, excluding labor cost, minor consumables, operational expenses (*e.g.* electricity and heating) and equipment depreciation, as we do not see them as drastically affecting the economics of the recycling process. In PSC manufacturing, equipment depreciation is the second largest cost contributor segment, accounting for about 18% of total costs according to ref. 35 and 37. However, the equipment for recycling is significantly less elaborate than the ones needed for fabrication. Our recycling process primarily utilized chromatography columns and a centrifuge, each costing less than 400 €, as well as a rotary evaporator, priced below 5000 €. Moreover, all these devices demand minimal labor and energy for operation. The exact cost contributions of the equipment are dependent on their lifetimes; yet, even with a conservative assumption here, we consider the costs of depreciation, labor and energy for recycling to be insignificant compared to materials.

Material and cost projections are shown in Table 3. The presented analysis makes assumptions regarding material waste in device production. While small scale lab cells are produced with spin coating, this method is disregarded for production at scale due to its impracticality and high material waste (~90%).[53] Viable fabrication techniques at scale such as slot-die coating or roll-to-roll printing feature material waste ratios below 1%.[53] To account for waste from imperfect production yield, filtration, rinsing, pre/post-printing, *etc.*, we assume a 10% total material loss, with the exception of ITO glass. ITO glass is assumed to be reused at 100%. On the other hand, we applied the recycling yields documented in the laboratory to the cost analysis. The yields of $MAPbI_3$ and spiro-OMeTAD following anti-solvent crystallization and column chromatography, respectively, have the potential to increase when scaling up the process. However, since the extent of this increase is uncertain, we have assumed that the yields achieved here are equivalent to those for a 1 m^2 solar module. Given a 10% assumed material loss during module production and the corresponding recycling yield, the mass flow of the material through the process can be constructed, as shown in Fig. 9a. To maintain a constant material mass flow, losses are compensated for by introducing additional fresh materials. The total cost of one component C_{HC} for the preparation of a module with "topped-up" recycled materials, hereafter referred to as a 'hybrid module' is given by:

$$C_{HC} = C_R + (M_o - 0.9 \times M_o \times Y) \times P_V \quad (1)$$

where C_R is the cost to recycle the component from the original modules, M_o is the mass required of this component, Y is the process-specific recycling yield, and P_V is the price of virgin material. Values for the different materials and steps are found in Tables 2 and 3. Based on the calculated numbers, we can determine the reduced cost for one component and thus the cost for the corresponding layer in a module using recycled materials (details are described in the ESI† and Table S2). Since the yield of recycled ITO/SnO_2 is 100% and they were used directly in cell fabrication, the cost of ITO and SnO_2 for one

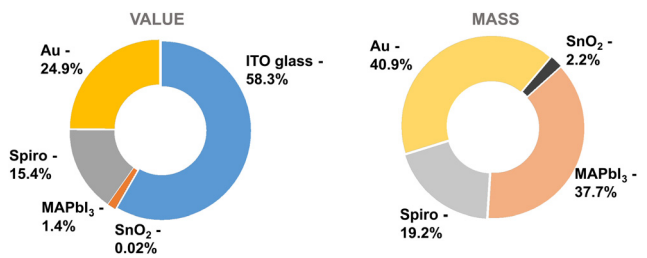

Fig. 7 Value (left) and mass (right) composition of the investigated perovskite solar device. Note that the mass of the sample is dominated by that of the ITO glass, which per area weighs 1000 times more than all other materials combined.

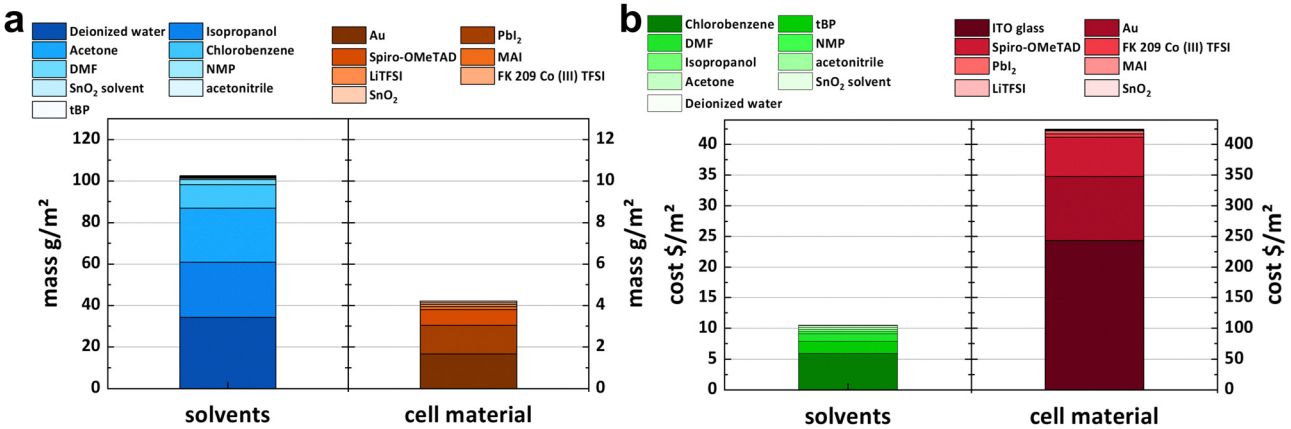

Fig. 8 (a) Mass and (b) value distribution of solvents used in the fabrication process (left) and materials used to make the cell (right). Note that the scales differ by a factor of 10.

Table 3 Chemical consumption and costs during the recycling process scaled for a perovskite module with 1 m^2 area based on our fabrication sequence with an active area of 70%. The solvent consumption for $MAPbI_3$ and spiro-OMeTAD was determined by their respective solubility, about 500 mg mL^{-1} $MAPbI_3$ in GBL,[54] and 367 mg mL^{-1} spiro-OMeTAD in chlorobenzene.[55] A 10% material loss during device fabrication is assumed. Each gram of material requires 20 g silica and 200 ml eluent during column chromatography. The amount of ethyl acetate should be about 3 times greater than that of GBL (as described in the ESI). The pricing was derived from our laboratory's procurement data (the source of the materials can be found in the ESI), with the exchange rate of 1 euro equivalent to 1.08 dollars, with an exception of the price of H_2O.[35] We are utilizing the yield data collected in our experiments for the 1 m^2 module

Target material	Material on stack	Chemical	Usage	Virgin material price ($)	Subtotal cost ($)	Total cost ($) [$C_R$]	Yield [Y]
SnO_2 + ITO glass	0.078 g + 5 kg	Ethanol	33 mL	27.97/2.5 L	0.37	0.54	100%
		SnO_2 (15%)	0.58 g	88.29/500 g	0.10		
		Deionized water	1.25 mL	0.012/L	0.00002		
		Isopropanol	1.25 mL	28.78/500 mL	0.072		
$MAPbI_3$	1.368 g	GBL	3.05 g	38.45/500 g	0.23	1.22	87%
		Ethyl acetate	8.2 mL	120.96/1 L	0.99		
Spiro-OMeTAD	0.697 g	Chlorobenzene	1.9 mL	137.98/250 mL	1.05	5.95	66%
		Silica gel	14 g	83.16/1 kg	1.16		
		Dichloromethane	133 mL	64.15/2.5 L	3.41		
		Ethyl acetate	7 mL	117.72/2.5 L	0.33		

hybrid module equals the cost to recycle them from one module.

Fig. 9b compares the cost of a 1 m^2 module constructed with exclusively virgin materials *versus* one hybrid module made with recycled materials (recycled ITO/SnO_2, $MAPbI_3$ and spiro-OMeTAD) and top-up virgin materials. The results show that a hybrid module produced on lab-scale incurs a significant cost reduction of 63.7% compared to the device made from virgin materials exclusively. Cost savings are mainly attributable to the savings from ITO glass and spiro-OMeTAD.

The potential for substantial cost- and material savings due to recycling practices in research laboratories is considerable. Our group operates two laboratories in Erlangen, i-MEET at the university of Erlangen-Nuremberg and high throughput methods in photovoltaics (HTM PV) in the Helmholtz Institute Erlangen-Nürnberg, focusing on photovoltaics research. The labs, housing approximately 50 researchers focusing on experiments, incurred materials expenses exceeding 0.22 million euros in 2021 and 2022 (more details can be found in Table S3, ESI†). TCO glass substrates, accounting for 7.5% of this expenditure, were notable contributors. Traditionally disposed of after use, these materials generate significant waste and associated management costs. Specifically, i-MEET produced 2190 liters of waste, equivalent to about 37 sixty-liter barrels, while HTM PV generated 827 kilograms, managed at a cost of 3758 euros (Table S3, ESI†). Waste management details for i-MEET are integrated with broader university operations, obscuring specific costs. Across 2021 and 2022, the cumulative publication output for organic and perovskite photovoltaics research, both reliant on TCO glass substrates, totals approximately 20 000 papers,[56] with our labs in Erlangen contributing around 50. Linear extrapolation suggests a global research community expenditure in the range of a hundred million euros on materials for perovskite- and organic solar cells alone.

Our research has highlighted the feasibility of recycling several of the materials involved, underlining the economic and material retention advantages that recycling can confer. We posit that this study serves as a compelling impulse for research laboratories engaged in research of perovskite and organic materials to incorporate recycling protocols into their

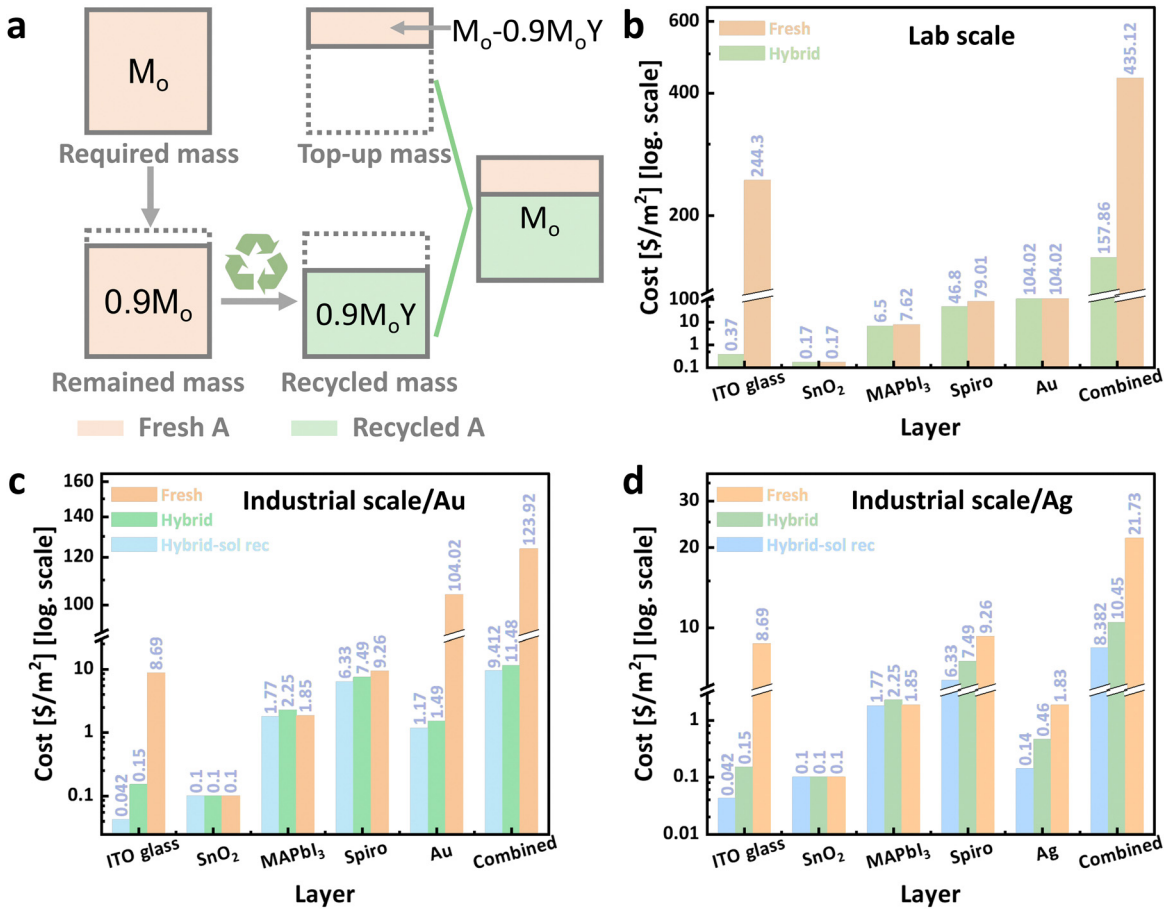

Fig. 9 (a) Mass flow of one component through production, recycling and reconstruction of one device; cost comparison of a 1 m^2 solar device using exclusively fresh materials (denoted as fresh), one using recycled materials and top-up fresh materials (denoted as hybrid), and one using recycled materials with solvents used in recycling process recycled and top-up fresh materials (denoted as hybrid-sol rec): (b) at a lab scale, (c) at an industrial scale with Au as back electrode, and (d) at an industrial scale with Ag as back electrode.

practices, thereby enhancing their environmental stewardship on the path toward sustainable technology.

Maximum recycling cost and minimum recycling yield. Based on eqn (1), we can calculate the maximum recycling cost and minimum recycling yield such that the use of hybrid recycled material should be preferred to that of virgin material. When the cost of a component for a hybrid module (C_{HC}) equals the cost of a virgin component required for one module (C_{VC}), the recycling process ceases to be economically interesting. Using the achieved recycling yields (66% for spiro-OMeTAD and 87% for $MAPbI_3$), we calculated the maximum sustainable recycling costs for spiro-OMeTAD and $MAPbI_3$ as 38.16 \$ and 2.34 \$, respectively. Conversely, fixing the recycling cost allows determination of the minimum sustainable recycling yields—10.3% for spiro-OMeTAD and 79.6% for $MAPbI_3$. For ITO glass, since there is no material waste in device production, eqn (1) requires adjustments for threshold calculations as below:

$$C_{HC} = C_R + (A_o - A_o \times Y) \times P_V \quad (2)$$

where A_o is the module area (1 m^2). Given the low threshold for re-using glass ITO glass, we find the use of almost any amount of recycled glass (>0.2%) is beneficial. The maximum recycling cost is 243.7 \$. With our approach, a whole fresh layer of SnO_2 was supplemented, leading to no profit, and thus is not discussed in this part. The thresholds of recycling cost and yield delineate a profitable region (shaded in blue in Fig. 10). More profitable recycling occurs toward the lower right corner of this region, where both yield is higher and cost is lower (represented by the deeper blue shading). The data points plotted within the blue regions represent our estimated recycling yields and costs for the components from Table 3. The positioning of spiro-OMeTAD and ITO glass within the darker blue areas indicates their recycling processes are economically attractive, especially in the case of ITO glass.

Industry-scale recycling. Should perovskite photovoltaics enter the commercial market, their recycling would likely become obligatory and essential. Yet, questions remain regarding the economic feasibility and incentives for industrial recycling of these materials.

Here we present a projection of how our recycling approach would translate to an industrial scale. A first step requires estimating material prices at scale. For this purpose, we project a growth in material demand by a factor of ten thousand. Material pricing was based on previous literature and assumes

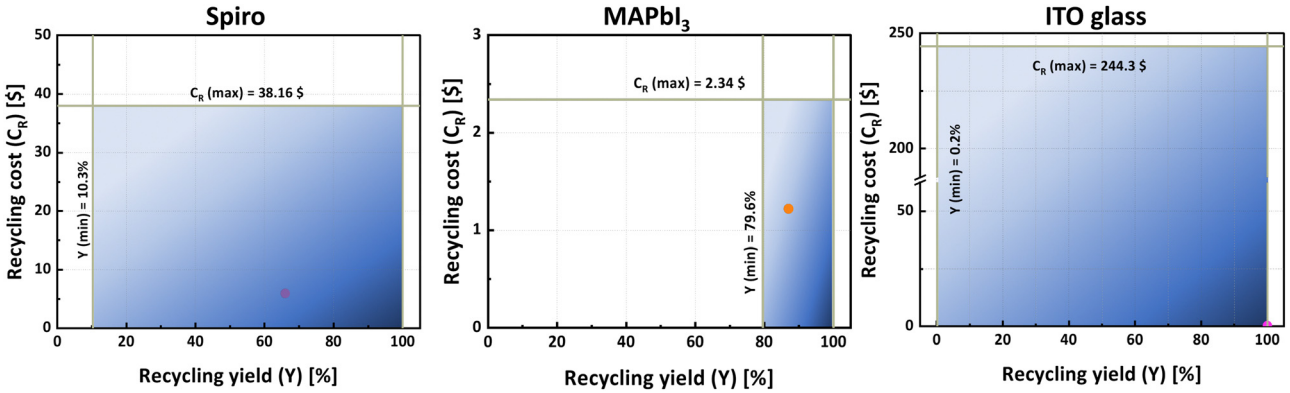

Fig. 10 Profitability analysis: theoretical thresholds and profitable regions for recycling process viability. Profit margins increase as the shade of blue deepens. The data points represent the estimated values in our case.

a 10% price-learning rate per volume doubling,[36] where suitable. For metal contacts and glass, price learning was not considered a viable approach. At an industrial scale, the ample availability of recovered metal electrodes eliminates the restriction of reuse imposed by the limited quantity of recovered electrodes at the lab scale. And a near-perfect electrode recycling rate is assumed for both thermal evaporation losses and solar panels. Gold is included for consistency, but an industrial process is assumed to use silver to achieve competitive cost, instead. We initially considered using carbon electrodes, as suggested earlier. However, the production of carbon pastes has not been upscaled yet, their price remains high (6.37 $ per g based on our laboratory's procurement data). As their required mass is large (14.38 g m^{-2}),[57] the current cost of carbon paste for a 1 m^2 module stands at 91.6 $—only marginally less than what gold electrodes would cost (104.02 $, presented in Table 2). Furthermore, the potential for cost reduction in carbon electrodes with mass production is uncertain. In contrast, silver electrodes are extensively utilized in the silicon PV industry, offering a more reliable analysis. Consequently, we decided to opt for silver electrodes. Glass production is already at scale and only minor effects are expected from additional scaling. Yet, for the lab process specially fabricated and therefore expensive glass substrates are used. In industrial processing, costs for the glass substrate are replaced by values that are in line with industrial scale cost models.[37] Additional assumptions are also made for the hole transport material. In our lab process, a comparatively expensive spiro-OMeTAD was used. In the projected industrial process, we assume that a more sustainable and cost-effective synthesis method for spiro-OMeTAD is adopted.[49]

Solvent recycling presents an additional opportunity for mitigating carbon emissions and enhancing economic returns. In our analysis, we incorporated a second scenario wherein solvents undergo recycling and subsequent reuse, with a 90% solvent reuse rate assumed. The recycled solvents are completely replaced with fresh solvents at regular intervals of every 5 m^2 of solar panels. Materials cost projections for the industrial process with and without recycling are shown in Fig. 9c and d, whereas the bar in the middle corresponds to the use of hybrid materials only, and the bar on the left corresponds to the use of recycled solvents as well. Fig. 9c shows the direct correspondence to our lab process with a gold electrode at 123.92 $ per m^2 materials cost, while Fig. 9d shows the analysis for silver with 21.73 $ per m^2. Incorporating recycled materials into a module (hybrid module) reduces the cost in all cases. As gold dominates the cost and gold can be recycled with great efficiency, cost savings due to recycling are substantial and amount to 90.7% without solvent reuse and 92.4% with. Replacing gold with silver removes the electrode as the dominating cost factor. Consequently, savings in material costs are smaller for the module with silver electrode, yet they still amount to 51.9% without solvent reuse and 61.4% with. These results show that a substantial economic benefit should be possible by adopting suitable recycling procedures.

Beyond differences in material prices and electrodes, encapsulation is another critical factor distinguishing lab settings from industrial settings in solar module production. Encapsulation is essential in industrial applications to extend module lifespan. The impact of encapsulation on recycling varies with the method and materials used. For example, an epoxy resin with a back cover glass is a highly likely structure for perovskite solar modules due to its superior stability.[30] Such encapsulants can be efficiently delaminated through a brief thermal treatment at an elevated temperature (250 °C for 2 min),[30] which consumes minimal energy and, consequently, minimal capital. Besides conventional methods, it is possible to design encapsulation techniques specifically to facilitate delamination, enabling easier recycling. Ideally, these methods would allow physical separation of the encapsulant without heating, such as direct removal, which consumes almost no energy. Overall, with the appropriate choice of encapsulation materials and techniques, the impact on recycling and associated costs should be manageable or even negligible.

Detailed price projections for the scaled process are given in the ESI† in Table S4, the industrial-scale costs for manufacturing a 1 m^2 panel are given in detail in Table S5 (ESI†), recycling costs are detailed in Table S6 (ESI†), and the costs for hybrid layers are given in Table S7 (ESI†). Table S8 (ESI†) presents the recycled mass of each component from a 1 m^2 module using our recycling method, in comparison to the mass of each

component on the module. The data indicates that 99.97% of the module mass can be recycled; a figure that significantly exceeds the European Union's mandated threshold of 80%.[9]

3.3 Life cycle assessment

A life cycle assessment was carried out to understand the carbon and environmental savings from recycling. In the assessment, we adopt the scenario where silver is the electrode and the solvents utilized for recycling is recycled. We define the system boundary to include three lifecycle stages: (1) raw material acquisition, (2) product fabrication, and (3) end of life, recycling in this case. The system boundary excludes the operation phase, in alignment with assumptions documented in existing literature.[22]

In this study, all recycled materials required processing before incorporation into cells, albeit to varying extents. ITO/SnO_2 was successfully recovered; however, it necessitated an additional fresh SnO_2 layer to restore device performance, which means it undergoes the same processing steps as virgin ITO/SnO_2. Similarly, spiro-OMeTAD could be recycled, but its processing procedures mirrored those of its virgin counterpart. The recycling of $MAPbI_3$ eliminated the need to weigh PbI_2 and MAI, a process that, in any case, consumes minimal energy. Thus, it is assumed that the fabrication of hybrid modules does not lead to carbon and environmental savings.

Recycling perovskite solar modules using the developed method minimally impacts the carbon footprint, as evidenced by low electricity and material consumption. Documented in Table S9 (ESI†), the electricity requirement for recycling is 4.81 kW h, a figure reflective of processing volumes potentially less than those from a 1 m^2 module (detailed in 'Material on stack' column in Table 3). Despite this ambiguity, the material quantities required for 1 m^2, all under 1.5 g, comfortably fall within the operational capacities of the setups, suggesting negligible electricity variation when scaling to a 1 m^2 module. Moreover, the introduction of solvent recycling further underscores the low chemical consumption, detailed in 'usage [U_{SR}]' column in Table S6 (ESI†).

Assessing the carbon and environmental impact of materials reserved through recycling is crucial. This requires analyzing the carbon footprint and environmental costs associated with sourcing the raw materials for the investigated 1 m^2 module. We applied the ReCiPe methodology,[58] utilizing cumulative energy demand, 18 midpoint environmental impact categories, and three endpoint indicators to quantify these impacts. The data, adapted from Tian *et al.*,[22] are presented in Tables S10 and S11 (ESI†). We can then determine the cumulative energy demand for all the materials required for the module to be 308 MJ m^{-2}. With Germany's average emissions standing at 354 g CO_2eq. per kW h in 2023,[59] the production of materials for a 1 m^2 module results in emissions of approximately 30 288 CO_2eq. Fig. S12 (ESI†) illustrates the breakdown of the cumulative energy demand for these materials, highlighting that ITO glass is the predominant contributor, accounting for 94.9% of the total. Fig. S13 (ESI†) illustrates the environmental profile of a 1 m^2 module based on the midpoint and endpoint indicators, underscoring that ITO glass not only dominates the energy demand but also has the largest environmental impact, followed by silver. Therefore, the developed recycling approach, which can retain ITO glass and more, could significantly reduce both carbon emissions and environmental impact.

4 Conclusion

Developing closed-loop recycling procedures to reduce material demand and avoid waste is one of the most important current tasks for photovoltaics. Solution-processed solar cells here have unique advantages over established technologies due to the possibility to dissolve materials selectively. In this work, we demonstrate the closed-loop recycling of planar perovskite solar cell with $MAPbI_3$ absorber. To demonstrate recyclability, we propose a procedure *via* the use of large area (125 mm × 85 mm) pseudo-modules to address material handling challenges and reduce material losses. From the pseudo-modules, we selectively and sequentially remove all layers of the solar cell stack from the substrate and recover the corresponding materials in solutions. The recovered materials are then purified and used to fabricate functional, small-scale (25 mm × 25 mm) solar cells where one, several, or all of the functional layers were made of recycled materials. Recovering ITO/SnO_2 substrates required the additional deposition of a thin layer (~20 nm) of fresh SnO_2 to repair damage incurred to the substrate. The additional layer boosted fill factors from 60% to 75%. We also recovered the gold electrode, yet the adopted metal evaporation process in our lab was found to be unsuitable for recycling. Comparing the efficiencies of our recycled solar cells with those of solar cells made of virgin materials verifies the effectiveness of the adopted process. In all combinations of virgin and recycled materials, efficiencies at similar levels between 17.1% and 17.6% were achieved.

Analysis of the value and mass distribution for all components used in processing of our lab-made solar cells revealed that ITO glass carries both the highest economic value and material weight, making it a high priority for recycling with respect to economic viability and sustainability. An analysis of used by-product chemicals reveals the need for developing strategies for the circular use especially of cleaning agents like acetone, isopropanol, and water. Moreover, recycling has the potential to afford substantial cost savings in the lab and for industrial processing. At lab scale, recycling can reduce fabrication costs by 63.7% compared to a module that uses entirely fresh materials. At an industrial level, the recycling approach remains economically viable. Retaining the original gold electrode results in a 90.7% cost reduction *versus* a fresh module, while substituting with silver affords savings of 51.9%. When reusing solvents, the reductions increase to 92.4% and 61.4% for gold and silver electrodes, respectively. The estimated recyclable mass fraction amounts to 99.97%, suggesting a significant savings potential for resources and landfill space. A life cycle assessment demonstrated the developed recycling approach can reduce carbon emissions and other environmental impacts.

Author contributions

Zhenni Wu: conceptualization, data curation, formal analysis, validation, investigation, visualization, methodology, writing – original draft, writing – review & editing. Mykhailo Sytnyk: conceptualization, data curation, formal analysis, investigation, methodology, writing – review & editing. Jiyun Zhang: data curation, validation, investigation, methodology, writing – review & editing. Gülüsüm Babayeva: investigation, writing – review & editing. Christian Kupfer: software, formal analysis, methodology, writing – review & editing. Jin Hu: investigation. Simon Arnold: investigation, writing – review & editing. Jens Hauch: resources, supervision, funding acquisition, writing – review & editing. Christoph Brabec: conceptualization, resources, supervision, funding acquisition, project administration, writing – review & editing. Ian Marius Peters: conceptualization, resources, supervision, funding acquisition, project administration, writing – original draft, writing – review & editing.

Conflicts of interest

There are no conflicts of interest to declare.

Acknowledgements

This work was supported by project Zeitenwende, VIPERLAB European Union's Horizon 2020 No. 101006715, Pero4PV (FKZ: 03EE1092A), Helmholtz Association in the framework of the innovation platform "Solar TAP" (Az: 714-62150-3/1 (2023)), "ELF-PV Design and development of solution processed functional materials for the next generations of PV technologies" (No. 44-6521a/20/4), and project "PV-Tera – Reliable and cost efficient photovoltaic power generation on the Terawatt scale" (No. 44-6521a/20/5) by the Bavarian State Government. Co-funded by the European Union (ERC, C2C-PV, project number 101088359). Views and opinions expressed are however those of the author(s) only and do not necessarily reflect those of the European Union or the European Research Council. Neither the European Union nor the granting authority can be held responsible for them. We appreciate Leonie Brandner, Corina Winkler, Nidia Gawehns and Erika Geffel for providing lab annual expenses on chemical purchases and chemical waste management data.

References

1 International Energy Agency. CO_2 Emissions in 2022. https://www.iea.org/reports/co2-emissions-in-2022 (accessed July 2023).
2 Intergovernmental Panel on Climate Change. Climate Change 2022: Mitigation of Climate Change. https://www.ipcc.ch/report/ar6/wg3/ (accessed July 2023).
3 World has installed 1TW of solar capacity. https://www.pv-magazine.com/2022/03/15/humans-have-installed-1-terawatt-of-solar-capacity/ (accessed July 2023).
4 N. M. Haegel, P. Verlinden, M. Victoria, P. Altermatt, H. Atwater, T. Barnes, C. Breyer, C. Case, S. De Wolf, C. Deline, M. Dharmrin, B. Dimmler, M. Gloeckler, J. C. Goldschmidt, B. Hallam, S. Haussener, B. Holder, U. Jaeger, A. Jaeger-Waldau, I. Kaizuka, H. Kikusato, B. Kroposki, S. Kurtz, K. Matsubara, S. Nowak, K. Ogimoto, C. Peter, I. M. Peters, S. Philipps, M. Powalla, U. Rau, T. Reindl, M. Roumpani, K. Sakurai, C. Schorn, P. Schossig, R. Schlatmann, R. Sinton, A. Slaoui, B. L. Smith, P. Schneidewind, B. J. Stanbery, M. Topic, W. Tumas, J. Vasi, M. Vetter, E. Weber, A. W. Weeber, A. Weidlich, D. Weiss and A. W. Bett, *Science*, 2023, **380**, 39–42.
5 D. Bogdanov, M. Ram, A. Aghahosseini, A. Gulagi, A. S. Oyewo, M. Child, U. Caldera, K. Sadovskaia, J. Farfan, L. De Souza Noel Simas Barbosa, M. Fasihi, S. Khalili, T. Traber and C. Breyer, *Energy*, 2021, **227**, 120467.
6 E. Pursiheimo, H. Holttinen and T. Koljonen, *Renewable Energy*, 2019, **136**, 1119–1129.
7 J. C. Goldschmidt, L. Wagner, R. Pietzcker and L. Friedrich, *Energy Environ. Sci.*, 2021, **14**, 5147–5160.
8 G. A. Heath, T. J. Silverman, M. Kempe, M. Deceglie, D. Ravikumar, T. Remo, H. Cui, P. Sinha, C. Libby, S. Shaw, K. Komoto, K. Wambach, E. Butler, T. Barnes and A. Wade, *Nat. Energy*, 2020, **5**, 502–510.
9 Directive 2012/19/EU of the European Parliament and of the Council of 4 July 2012 on Waste Electrical and Electronic Equipment (WEEE) (recast) (European Commission, 2012). https://eur-lex.europa.eu/legal-content/EN/TXT/PDF/?uri=CELEX:32012L0019 (accessed July 2023).
10 EN50625-2-4:2017, Collection, logistics & treatment requirements for WEEE - Part 2–4: Treatment requirements for photovoltaic panels. CENELEC. https://www.cencenelec.eu/?p=104:110:124258077628101::::FSP_ORG_ID,FSP_PROJECT,FSP_LANG_ID:1258637,59265,25, 2017 (accessed July 2023).
11 Photovoltaic module stewardship and takeback program. RCW 70.355.010. Washington State Legislature. https://app.leg.wa.gov/RCW/dispo.aspx?cite=70.355.010, 2020. (accessed July 2023).
12 Preparation of a Recycling Scheme for Future Waste such as PV Panel (in Korean) (Korean Ministry of Environment). https://www.me.go.kr/home/web/board/read.do?menuId=286&boardMasterId=1&boardCategoryId=39&boardId=913050, 2018 (accessed July 2023).
13 Guidelines for Promoting Recycling of Solar Power Generation Equipment 2nd edn (Japanese Ministry of the Environment, 2018). https://www.env.go.jp/press/files/jp/110488.pdf. (accessed July 2023).
14 PV cycle annual report 2016. https://pvcycle.org/wp-content/uploads/2021/05/2016-Annual-Report-PV-CYCLE-AISBL.pdf. (accessed July 2023).
15 H. M. Wikoff, S. B. Reese and M. O. Reese, *Joule*, 2022, **6**, 1710–1725.
16 F. C. S. M. Padoan, P. Altimari and F. Pagnanelli, *Sol. Energy*, 2019, **177**, 746–761.
17 M. M. Lunardi, J. P. Alvarez-Gaitan, J. I. Bilbao and R. Corkish, in *Solar Panels and Photovoltaic Materials*, ed. B. Zaidi, InTechOpen, London, 2018, ch. 2, pp. 9–27.
18 R. Deng, N. L. Chang, Z. Ouyang and C. M. Chong, *Renewable Sustainable Energy Rev.*, 2019, **109**, 532–550.

19 R. G. Charles, A. Doolin, R. García-Rodríguez, K. Valadez Villalobos and M. L. Davies, *Energy Environ. Sci.*, 2023, **16**, 3711–3733.
20 Best Research-Cell Efficiencies. **https://www.nrel.gov/pv/cell-efficiency.html** (accessed July 2023).
21 T. D. Siegler, A. Dawson, P. Lobaccaro, D. Ung, M. E. Beck, G. Nilsen and L. L. Tinker, *ACS Energy Lett.*, 2022, **7**, 1728–1734.
22 X. Tian, S. D. Stranks and F. You, *Nat. Sustainable*, 2021, **4**, 821–829.
23 B. J. Kim, D. H. Kim, S. L. Kwon, S. Y. Park, Z. Li, K. Zhu and H. S. Jung, *Nat. Commun.*, 2016, **7**, 11735.
24 J. M. Kadro, N. Pellet, F. Giordano, A. Ulianov, O. Müntener, J. Maier, M. Grätzel and A. Hagfeldt, *Energy Environ. Sci.*, 2016, **9**, 3172–3179.
25 L. Huang, Z. Hu, J. Xu, X. Sun, Y. Du, J. Ni, H. Cai, J. Li and J. Zhang, *Sol. Energy Mater. Sol. Cells*, 2016, **152**, 118–124.
26 V. Larini, C. Ding, F. Faini, G. Pica, G. Bruni, L. Pancini, S. Cavalli, M. Manzi, M. Degani, R. Pallotta, M. De Bastiani, C.-Q. Ma and G. Grancini, *Adv. Funct. Mater.*, 2023, 2306040, DOI: **10.1002/adfm.202306040**.
27 H. Zhang and N.-G. Park, *eScience*, 2022, **2**, 567–572.
28 J. Xu, Z. Hu, L. Huang, X. Huang, X. Jia, J. Zhang, J. Zhang and Y. Zhu, *Prog. Photovolt. Res. Appl.*, 2017, **25**, 1022–1033.
29 C. G. Poll, G. W. Nelson, D. M. Pickup, A. V. Chadwick, D. J. Riley and D. J. Payne, *Green Chem.*, 2016, **18**, 2946–2955.
30 B. Chen, C. Fei, S. Chen, H. Gu, X. Xiao and J. Huang, *Nat. Commun.*, 2021, **12**, 5859.
31 S. Zhang, L. Shen, M. Huang, Y. Yu, L. Lei, J. Shao, Q. Zhao, Z. Wu, J. Wang and S. Yang, *ACS Sustainable Chem. Eng.*, 2018, **6**, 7558–7564.
32 A. Binek, M. L. Petrus, N. Huber, H. Bristow, Y. Hu, T. Bein and P. Docampo, *ACS Appl. Mater. Interfaces*, 2016, **8**, 12881–12886.
33 X. Feng, Q. Guo, J. Xiu, Z. Ying, K. W. Ng, L. Huang, S. Wang, H. Pan, Z. Tang and Z. He, *Cell Rep. Phys. Sci.*, 2021, **2**, 100341.
34 K. Wang, T. Ye, X. Huang, Y. Hou, J. Yoon, D. Yang, X. Hu, X. Jiang, C. Wu, G. Zhou and S. Priya, *Matter*, 2021, **4**, 2522–2541.
35 N. L. Chang, A. W. Y. Ho-Baillie, P. A. Basore, T. L. Young, R. Evans and R. J. Egan, *Prog. Photovoltaics*, 2017, **25**, 390–405.
36 N. L. Chang, A. W. Y. Ho-Baillie, D. Vak, M. Gao, M. A. Green and R. J. Egan, *Sol. Energy Mater. Sol. Cells*, 2018, **174**, 314–324.
37 Z. Song, C. L. McElvany, A. B. Phillips, I. Celik, P. W. Krantz, S. C. Watthage, G. K. Liyanage, D. Apul and M. J. Heben, *Energy Environ. Sci.*, 2017, **10**, 1297.
38 Y. Zhao, J. Zhang, Z. Xu, S. Sun, S. Langner, N. T. P. Hartono, T. Heumueller, Y. Hou, J. Elia, N. Li, G. J. Matt, X. Du, W. Meng, A. Osvet, K. Zhang, T. Stubhan, Y. Feng, J. Hauch, E. H. Sargent, T. Buonassisi and C. J. Brabec, *Nat. Commun.*, 2021, **12**, 2191.
39 J. Zhang, S. Langner, J. Wu, C. Kupfer, L. Lüer, W. Meng, B. Zhao, C. Liu, M. Daum, A. Osvet, N. Li, M. Halik, T. Stubhan, Y. Zhao, J. A. Hauch and C. J. Brabec, *ACS Energy Lett.*, 2021, **7**, 70–77.
40 N. A. N. Ouedraogo, G. O. Odunmbaku, B. Guo, S. Chen, X. Lin, T. Shumilova and K. Sun, *ACS Appl. Mater. Interfaces*, 2022, **14**, 34303–34327.
41 W. H. Nguyen, C. D. Bailie, E. L. Unger and M. D. McGehee, *J. Am. Chem. Soc.*, 2014, **136**, 10996–11001.
42 F. M. Rombach, S. A. Haque and T. J. Macdonald, *Energy Environ. Sci.*, 2021, **14**, 5161–5190.
43 E. V. Péan, S. Dimitrov, C. S. De Castroc and M. L. Davies, *Phys. Chem. Chem. Phys.*, 2020, **22**, 28345–28358.
44 C. Kupfer, V. M. Le Corre, C. Li, L. Lüer, K. Forberich, M. Kato, A. Osveta and C. J. Brabec, *J. Mater. Chem. C*, 2024, **12**, 95–102.
45 W. Chu, Q. Zheng, O. V. Prezhdo, J. Zhao and W. A. Saidi, *Sci. Adv.*, 2020, **6**, eaaw7453.
46 K. X. Steirer, P. Schulz, G. Teeter, V. Stevanovic, M. Yang, K. Zhu and J. J. Berry, *ACS Energy Lett.*, 2016, **1**, 360–366.
47 L. Qiu, S. He, L. K. Ono, S. Liu and Y. Qi, *ACS Energy Lett.*, 2019, **4**, 2147–2167.
48 J. Gong, S. B. Darling and F. You, *Energy Environ. Sci.*, 2015, **8**, 1953–1968.
49 S. Mattiello, G. Lucarelli, A. Calascibetta, L. Polastri, E. Ghiglietti, S. K. Podapangi, T. M. Brown, M. Sassi and L. Beverina, *ACS Sustainable Chem. Eng.*, 2022, **10**, 4750–4757.
50 Substance information of N,N-dimethylformamide, European Chemicals Agency. **https://echa.europa.eu/substance-information/-/substanceinfo/100.000.617** (accessed March 2024).
51 Substance information of 1-methyl-2-pyrrolidone, European Chemicals Agency. **https://echa.europa.eu/substance-information/-/substanceinfo/100.011.662** (accessed March 2024).
52 Substance information of chlorobenzene, European Chemicals Agency. **https://echa.europa.eu/substance-information/-/substanceinfo/100.003.299** (accessed March 2024).
53 N. Chaturvedi, N. Gasparini, D. Corzo, J. Bertrandie, N. Wehbe, J. Troughton and D. Baran, *Adv. Funct. Mater.*, 2021, **31**, 2009996.
54 M. I. Saidaminov, A. L. Abdelhady, G. Maculan and O. M. Bakr, *Chem. Commun.*, 2015, **51**, 17635–17778.
55 L. Yang, B. Xu, D. Bi, H. Tian, G. Boschloo, L. Sun, A. Hagfeldt and E. M. J. Johansson, *J. Am. Chem. Soc.*, 2013, **135**, 7378–7385.
56 O. Almora, D. Baran, G. C. Bazan, C. I. Cabrera, S. Erten-Ela, K. Forberich, F. Guo, J. Hauch, A. W. Y. Ho-Baillie, T. J. Jacobsson, R. A. J. Janssen, T. Kirchartz, N. Kopidakis, M. A. Loi, R. R. Lunt, X. Mathew, M. D. McGehee, J. Min, D. B. Mitzi, M. K. Nazeeruddin, J. Nelson, A. F. Nogueira, U. W. Paetzold, B. P. Rand, U. Rau, H. J. Snaith, E. Unger, L. Vaillant-Roca, C. Yang, H.-L. Yip and C. J. Brabec, *Adv. Energy Mater.*, 2024, **14**, 2303173.
57 P. Kajal, B. Verma, S. G. R. Vadaga and S. Powar, *Glob. Challenges*, 2022, **6**, 2100070.
58 M. Goedkoop, R. Heijungs, M. Huijbregts, A. De Schryver, J. Struijs and R. Van Zelm, ReCiPe 2008: A Life Cycle Impact Assessment Method Which Comprises Harmonised Category Indicators at the Midpoint and the Endpoint Level: Report 1: Characterisation, Ministry of Housing, Spatial Planning and Environment (VROM), 2009.
59 Emissions in Germany. **https://www.nowtricity.com/country/germany/**(accessed March 2024).

